Research Paper
Computational Methods for Differential Equations
http://cmde.tabrizu.ac.ir
Vol. *, No. *, *, pp. 1-14
DOI:10.22034/cmde.2026.66665.3137

An approximate solution of inverse source problem for the time-fractional diffusion equation

Settara Loubna[1,*], Atmania Rahima[2], and Mehri Allaoua[3]

[1]Lamahis Laboratory, Departement of Mathematics, University of 20 August 1955, Skikda , Algeria.

[2]LMA Laboratory, Department of Mathematics, University of Badji Mokhtar Annaba, P.O. Box 12, Annaba 23000, Algeria.

[3]LANOS Laboratory,Department of Mathematics, University of Chadli Bendjedid, El-Tarf 36000, Algeria.

Abstract

This paper investigates a one-dimensional inverse source problem associated with a time-fractional diffusion equation subject to Dirichlet boundary conditions. The primary focus is on analysing the differentiability of the source function and reformulating the inverse problem in terms of the invertibility input-output mapping. The novelty of the study lies in the characterization of these mappings under the Caputo derivative. To obtain approximate solutions we employ a finite difference scheme based on the $L1$ method. Numerical simulations demonstrate the accuracy and reliability of the proposed approach. Improving algorithmic efficiency will also be a focus of our future research.

Keywords. Time-fractional diffusion equation, Caputo fractional derivative, Inverse problem, Finite difference method, $L1$ method.

2010 Mathematics Subject Classification. 35R11, 65M32, 35R30, 65M06, 65L05.

1. Introduction

Fractional partial differential equations (FPDEs) have gained considerable attention in recent years, emerging as powerful tools for modelling and analysing the complex dynamics of systems in various scientific and engineering domains. From both theoretical and application-driven perspectives, FPDEs represent a rapidly evolving area of research. A comprehensive account of the theory of such equations can be found in existing monographs; see, for example, [17]. Consequently, fractional ordinary differential equations, fractional partial differential equations, and integral-equation formulations have attracted extensive interest. Many fractional differential equations, both linear and non-linear, do not admit closed-form analytical solutions; instead, approximations and numerical methods are commonly employed.

Several techniques have been developed to solve these types of equations in the literature, including the differential transformation method [18], iterative methods [8, 9, 13], and spectral methods [3, 4]. Recent surveys and reviews have summarized a variety of numerical methods and their convergence properties for FPDEs; see, for instance, [22].

Recent studies have also made significant progress in addressing inverse problems (ISPs), which play a critical role in a wide range of scientific and engineering applications, including geophysics, medical imaging, heat conduction, and electromagnetic field reconstruction. These problems aim to determine unknown source terms from indirect and often noisy observations of the system response. Their significance lies in their ability to provide insights into underlying physical processes that cannot be measured directly, which is essential for diagnostic, monitoring, and control purposes (see, e.g., [7, 14]). One of the key advantages of ISPs is their flexibility in modelling complex systems where internal sources cannot be accessed through direct measurement. They also offer a robust framework for data assimilation and system identification.

However, ISPs are typically ill-posed in the sense of Hadamard: small errors in the data may lead to large deviations in the reconstructed solution, thereby necessitating regularization techniques and careful numerical treatment (e.g.,

Received: 07 April 2025; Accepted: 27 April 2026.
∗ Corresponding author. Email: l.settara@univ-skikda.dz.

[15, 26]). Establishing the well-posedness of an inverse problem is therefore essential prior to developing numerical algorithms or performing simulations.

In recent years, inverse source problems for fractional diffusion equations have attracted increasing interest due to the ability of fractional models to capture memory and anomalous-diffusion effects commonly observed in complex media. The non-local nature of fractional derivatives introduces additional challenges in the analysis and numerical treatment of inverse problems, particularly when data are limited or contaminated by noise. Despite these difficulties, fractional inverse source problems have demonstrated strong potential in applications such as hydrology, viscoelasticity, and biomedical imaging, where classical integer-order models often fail to describe observed phenomena accurately [25]. Several studies have investigated the uniqueness, stability, and numerical reconstruction of source terms in time-fractional diffusion equations; see, for instance, [12, 21, 27]. Li and Yamamoto [19] have provided a rigorous analysis of identifiability under limited data.

Several recent contributions have advanced the numerical treatment of time-fractional inverse problems. For instance, the $L1$ method has emerged as a popular and efficient discretisation for Caputo fractional derivatives due to its simplicity and first-order convergence on uniform time grids [20]. Dehghan [1] developed efficient mesh-based methods for time-fractional diffusion equations with source identification, while Liu [6] proposed improved schemes offering enhanced accuracy and stability; see also [2, 11] for further developments. A relatively small body of research addresses inverse problems for time-fractional parabolic equations under various conditions. Numerical solutions for some of these problems have been discussed in [5, 23]. The present paper considers such problems as a generalization of the findings in [28]. The objective of this work is to investigate a time-fractional parabolic partial differential equation involving an inverse source term under non-homogeneous boundary conditions. An eigenfunction expansion of the corresponding Sturm–Liouville eigenvalue problem is employed to obtain an analytical representation, together with Dirichlet-type measured output data at the level of the fractional diffusion equation. The time-dependent inverse coefficient problem is analysed, and the distinguishability of the associated mappings is examined. In addition, an explicit expression for the input–output mapping—based on the measured data—is constructed. It is shown that the distinguishability of this mapping implies injectivity. To address the problem from a new perspective, a Fourier approach is adopted.

To introduce the input–output mapping $\Phi[\cdot] : \mathcal{K} \to C^1[0,T]$, where $\mathcal{K}$ denotes the set of admissible source functions, noisy Dirichlet data $E(t)$ are used to derive an analytical representation of the mapping. Using this formulation, we study the distinguishability of the unknown source function $c(t)$.

Finally, a finite-difference scheme is used to construct a numerical approximation of the problem. The modelling framework for the diffusion equation follows the approach described in [25].

The remainder of this paper is organized as follows. Section 2 establishes the mathematical foundation by reviewing key concepts in fractional calculus, including the Riemann–Liouville integral and the Caputo derivative, with particular emphasis on their non-local properties. Section 3 presents the theoretical core of this work: a novel Fourier-based approach for characterizing the injectivity of the input–output mapping $\Phi[\cdot]$. Section 4 introduces the $L1$ finite-difference scheme used to address numerical stability in time-fractional problems. Practical examples are provided to validate the robustness of the theoretical results and the efficiency of the numerical implementation. The final section provides concluding remarks.

2. Basic concepts of fractional calculus

This section provides essential concepts and notations that are crucial for understanding the paper's main ideas, for additional informations see [24].

Definition 2.1. The left-sided Riemann-Liouville fractional integral of order $0 < \alpha < 1$ of $f \in L^1(a,T)$ is defined by

$$I^{\alpha}_{a+} f(t) := \frac{1}{\Gamma(\alpha)} \int_a^t \frac{f(s)}{(t-s)^{1-\alpha}} ds, \quad t > 0, \tag{2.1}$$

where $\Gamma(\alpha)$ is the Euler gamma function.

Definition 2.2. The Caputo fractional derivative of order α of the function $f : \mathbb{R}^+ \longrightarrow \mathbb{R}$ is defined as

$$ {}^{C}D_0^{\alpha} f(t) = \frac{1}{\Gamma(n-\alpha)} \int_0^t (t-s)^{n-\alpha-1} f^{(n)}(s) ds = I^{n-\alpha} f^{(n)}(t), \tag{2.2}$$

where $n-1 < \alpha \leq n$ and $n = [\alpha] + 1$ with $[\alpha]$ the integer part of α.

Proposition 2.3. *The Euler gamma function $\Gamma(z)$ satisfies the following properties:*

$$\Gamma(z+1) = z\,\Gamma(z), \tag{2.3}$$

$$\int_0^1 s^{z-1}(1-s)^{w-1}\, ds = \frac{\Gamma(z)\,\Gamma(w)}{\Gamma(z+w)}, \quad z, w > 0. \tag{2.4}$$

Definition 2.4. The two-parameter Mittag–Leffler function is defined by the series

$$E_{\alpha,\beta}(z) = \sum_{n=0}^{\infty} \frac{z^n}{\Gamma(\alpha n + \beta)}, \quad \alpha, \beta, z \in \mathbb{C},\ \Re(\alpha) > 0. \tag{2.5}$$

In particular, if $\beta = 1$, then $E_{\alpha,1}(z) = E_{\alpha}(z)$; and if $\alpha = \beta = 1$, then $E_1(z) = e^z$.

3. Formulation and analysis of the inverse source problem with measured Data $E(t)$

We consider the following inverse source problem for a time-fractional partial differential equation with boundary and initial conditions:

$$ {}^{C}D_{0^+,t}^{\alpha} u(x,t) - u_{xx}(x,t) + q(x)u(x,t) = c(t)f(x), \qquad 0 < \alpha \leq 1,\ (x,t) \in \Omega_T, \tag{3.1}$$

$$u(x,0) = \varphi(x), \qquad 0 < x < 1, \tag{3.2}$$

$$u(0,t) = \psi_1(t), \quad u(1,t) = \psi_2(t), \qquad 0 < t < T, \tag{3.3}$$

where $\Omega_T = \{(x,t) \in \mathbb{R}^2 : 0 < x < 1, 0 < t \leq T\}$. The boundary functions $\psi_1(t)$ and $\psi_2(t)$ belong to $C[0,T]$, and the functions $q(x)$ and $\varphi(x)$ satisfy the following conditions:

(A_1) $q(x) \in C^1[0,1]$, $0 < c_0 \leq q(x) < c_1$,
(A_2) $\varphi(x) \in C^2[0,1]$, $\varphi(0) = \psi_1(0)$, $\varphi(1) = \psi_2(0)$.

Under these assumptions, the problem (3.1) has a unique solution $u(x,t) \in C(\Omega_T) \cap W_t^1(0,T) \cap C_x^2(0,1)$ that satisfies the equation, initial, and boundary conditions. Here $W_t^1(0,T)$ denotes the space of functions $\chi \in C^1(0,T)$ with $\chi' \in L(0,T)$.

The inverse problem consists of determining the unknown source function $c(t)$ at a spatial point $x = x_0$ from the measured output data

$$E(t) = u(x_0, t; c). \tag{3.4}$$

We define the input-output mapping

$$\Phi[c] = u(x_0, t; c), \quad c \in \mathcal{K} \subset L^1(0,T), \tag{3.5}$$

so that the inverse problem reduces to determining $c(t)$ from $\Phi[c]$. The mapping Φ is said to have the *distinguishability property* if

$$\Phi[c_1] \neq \Phi[c_2] \implies c_1(t) \neq c_2(t), \quad \forall c_1, c_2 \in \mathcal{K}. \tag{3.6}$$

with this strategy, the problem of input-output mapping's invertibility $\Phi[.]$ replaces the inverse problem of determining an unknown $c(t)$. This prompts us to use the input-output mapping mentioned above to verify the source function's uniqueness. We state that the $\Phi[.]$ mapping if $\Phi[c_1] \neq \Phi[c_2]$, then has the distinguishability property. Then, $c_1(t) \neq c_2(t)$ is implied. This specific meaning of injectivity of Φ^{-1} is the inverse mapping. Examine the inverse problem using the measured $E(t)$ output data. Therefore, using the input-output mapping mentioned above, we can verify that the

source function is unique. We provide an auxiliary function $\Theta(x,t)$ to be able to develop the solution for parabolic problem (3.1)by the Fourier technique of separation of variables as follows

$$\Theta(x,t) = u(x,t) - (1-x)\psi_1(t) - x\psi_2(t), \tag{3.7}$$

by which the problem (3.1) is changed to one with homogenous boundary conditions. As a result, $\Theta(x,t)$ can be used to describe the initial value problem as follows.

$$\begin{aligned} {}^{C}D_t^{\alpha}\Theta(x,t) - \Theta_{xx}(x,t) &= -q(x)\Theta(x,t) + xq(x)\psi_2(t) + (1-x)q(x)\psi_1(t) \\ &\quad - x\,{}^{C}D_t^{\alpha}\psi_2(t) - (1-x)\,{}^{C}D_t^{\alpha}\psi_1(t) + c(t)f(x), \qquad (3.8)\\ \Theta(x,0) &= \varphi(x) - (1-x)\psi_1(0) - x\psi_2(0), \qquad (3.9)\\ \Theta(0,t) &= \Theta(1,t) = 0. \qquad (3.10) \end{aligned}$$

For the initial boundary value problem, the specific solution is as follows

$$\begin{aligned} \Theta(x,t) &= \sum_{n=1}^{+\infty} \langle H(\theta), X_n(\theta)\rangle\, E_{\alpha,1}(-\lambda_n t^{\alpha}) X_n(x) + \sum_{n=1}^{+\infty} \int_0^t s^{\alpha-1} E_{\alpha,\alpha}(-\lambda_n) s^{\alpha} \langle h(\theta, t-s), X_n(\theta)\rangle\, X_n(x) ds \\ &\quad + \sum_{n=1}^{+\infty} \int_0^t s^{\alpha-1} E_{\alpha,\alpha}(-\lambda_n) s^{\alpha} c(t-s) \langle f(\theta), X_n(\theta)\rangle\, ds X_n(x), \end{aligned} \tag{3.11}$$

where

$$H(x) = \varphi(x) - (1-x)\psi_1(0) - x\psi_1(0), \tag{3.12}$$

and

$$h(x,t) = -q(x)v(x,t) + xq(x)\psi_2(t) + \psi_1(t) - x\psi_1(t) - xD_t^{\alpha}\psi_2(t) - (1-x)D_t^{\alpha}\psi_1(t). \tag{3.13}$$

Moreover

$$< H(\theta), X_n(\theta) >= \int_0^1 X_n(\theta) H(\theta) d\theta, \tag{3.14}$$

$E_{\alpha,\beta}$ being the generalized Mittag-Leffler function defined by Eq. (2.5).

Assume that the following Sturm-Liouville [19] has a solution represented by $X_n(x)$.

$$\begin{cases} -X_{xx}(x) = \lambda X(x) + q(x)X(x), & 0 < x < 1, \\ X(0) = X(1) = 0, & 0 < t < T. \end{cases} \tag{3.15}$$

The measured output data's Dirichlet type can be expressed in the manner shown below.

$$E(t) = \Theta(x_0,t) + (1-x_0)\psi_1(t) + x_0\psi_2(t). \tag{3.16}$$

In order to arrange Eq. (3.11), let's clarify the subsequent

$$z_n(t) =< H(\theta), X_n(\theta) > E_{\alpha,1}(-\lambda_n t^{\alpha}). \tag{3.17}$$

$$w_n(t) = \int_0^t s^{\alpha-1} E_{\alpha,\alpha}(-\lambda_n) s^{\alpha} < H(\theta, t-s) q_j, X_n(\theta) > ds. \tag{3.18}$$

$$\gamma_n(t) = \int_0^t s^{\alpha-1} E_{\alpha,\alpha}(-\lambda_n) s^{\alpha} c(t-s) < f(\theta), X_n(\theta) > ds. \tag{3.19}$$

The following form can be used to express the resolution in terms of $z_n(t), w_n(t)$ and $\gamma_n(t)$, see [16] for further information.

$$\Theta(x,t) = \sum_{n=1}^{\infty} z_n(t)X_n(x) + \sum_{n=1}^{\infty} w_n(t)X_n(x) + \sum_{n=1}^{\infty} \gamma_n(t)X_n(x). \tag{3.20}$$

The analytical solution of the problem (3.1)-(3.15) in series form is given in Eq. (3.20). Therefore,

$$E(t) = \sum_{n=1}^{\infty} z_n(t)X_n(x_0) + \sum_{n=1}^{\infty} w_n(t)X_n(x_0) + \sum_{n=1}^{\infty} \gamma_n(t)X_n(x_0)dx + (1-x_0)\psi_1(t) + x_0\psi_2(t), \tag{3.21}$$

is acquired. Consequently, $E(t)$ can be found analytically as a series representation Eq.(3.21) on the right-hand side describes the input-output mapping $\Psi[c]$.

$$\Psi[c](t) : \sum_{n=1}^{\infty} z_n(t)X_n(x_0) + \sum_{n=1}^{\infty} w_n(t)X_n(x_0) + \sum_{n=1}^{\infty} \gamma_n(t)X_n(x_0)dx + (1-x_0)\psi_1(t) + x_0\psi_2(t). \tag{3.22}$$

The relation between the corresponding outputs $E_j(t) = u(x_0,t,c_j), j = 1,2$ and the source functions $c_1(t), c_2(t) \in \mathcal{K}$ at x_0 is implied by the following lemma.

Lemma 3.1. *[23] The solutions to the direct issue (3.1) and $\upsilon_2(x,t) = \upsilon(x,t;c_2)$ should be considered. These correspond to the admissible coefficients $c_1(t), c_2(t) \in \mathcal{K}$. If the corresponding outputs $E_j(t) j = 1,2$ fulfil the following series identity, then $E_j(t) = u(x_0,t;c_j); j = 1,2$.*

$$\Delta E(t) = \sum_{n=1}^{+\infty} \Delta w_n(t)X_n(x_0) + \sum_{n=1}^{+\infty} \Delta\gamma_n(t)X_n(x_0), \tag{3.23}$$

for each $t \in (0,T]$ where $\Delta E(t) = E_1(t) - E_2(t), \Delta w_n(t) = w_n^1(t) - w_n^2(t), \Delta\gamma_n(t) = \gamma_n^1(t) - \gamma_n^2(t)$.

Proof. By using identity Eq.(3.21), the measured output data $E_j(t) = \Theta(x_0,t); j = 1,2$ can be expressed as

$$E_1(t) = \sum_{n=1}^{+\infty} z_n^1(t)X_n(x_0) + \sum_{n=1}^{+\infty} w_n^1(t)X_n(x_0) + \sum_{n=1}^{+\infty} \gamma_n^1(t)X_n(x_0) + (1-x_0)\psi_1(t) + x_0\psi_2(t), \tag{3.24}$$

$$E_2(t) = \sum_{n=1}^{+\infty} z_n^2(t)X_n(x_0) + \sum_{n=1}^{+\infty} w_n^2(t)X_n(x_0) + \sum_{n=1}^{+\infty} \gamma_n^2(t)X_n(x_0) + (1-x_0)\psi_1(t) + x_0\psi_2(t), \tag{3.25}$$

respectively, since $z_n^1 = z_n^2$ from the definition of $z_n(t)$. The difference between Eqs. (3.24)-(3.25) implies the intended outcome. □

We arrive at the following conclusion as a result of the definitions and lemma.

Corollary 3.2. *Let the conditions of lemma 3.1*

$$< c_1(t) - c_2(t), X_n(x) >= 0, \forall t \in (0,T], n = 0,1,\ldots, \tag{3.26}$$

holds, then

$$E_1(t) = E_2(t), \forall t \in [0,T]. \tag{3.27}$$

Theorem 3.3. *Assume $(A_1) - (A_2)$.Let $\Phi[.] : \mathcal{K} \to C^1[0,T]$ Equation (3.22) defines the input-output mapping, which corresponds to the measured output $E(t) = u(x_0,t)$.Under the class of admissible parameters $\mathcal{K}$, the mapping $\Phi[c]$ in this instance possesses the distinguishability property, that is,*

$$\Phi[c_1] \neq \Phi[c_2] \Rightarrow c_1(t) \neq c_2(t), \forall c_1, c_2 \in \mathcal{K}. \tag{3.28}$$

Proof. If $c_1(t) \neq c_2(t)$ implies $\langle c_1(t) - c_2(t), X_n(x)\rangle \neq 0$ and $\Delta\gamma_n(t) \neq 0$, for some $n \in \mathbb{N}$, hence by Lemma 3.1 we conclude that $E_1(t) \neq E_2(t), \forall t \in [0,T]$. Moreover, it leads us to the following important consequence that the input-output mapping $\Phi[c]$ is distinguishable, i-e.$c_1(t) \neq c_2(t)$ implies $\Phi(c_1) \neq \Phi(c_2)$. □

4. Numerical procedure

In this section, we discretize the problem (3.1) using the finite difference method. Let the spatial step $h = \frac{1}{M}$ and the time step size $\Delta t = \frac{T}{N}$, where M, N are positive integers. The domain $[0,1] \times [0,T]$ is divided into a mesh $M \times N$, with grid points

$$x_i = ih,\ t_j = j\Delta t,\ i = 0, ..., M,\ \ j = 0, ..., N.$$

For the Caputo derivative ${}^{C}D_t^{\alpha} u(x_i, t_j)$ with $0 < \alpha < 1$ [10], we use the $L1$ approximation

$$
\begin{aligned}
{}^{C}D_t^{\alpha} u(x_i, t_j) &= \frac{1}{\Gamma(1-\alpha)} \int_0^{t_j} (t_j - s)^{-\alpha} \frac{\partial u}{\partial t}(x_i, s) ds && (4.1)\\
&\simeq \frac{1}{\Gamma(2-\alpha)} \sum_{k=0}^{j-1} \left[(j-k)^{1-\alpha} - (j-\alpha-1)^{1-\alpha}\right] \left[\frac{u_j^{k+1} - u_j^k}{(\Delta t)^{\alpha}}\right] && (4.2)\\
&= \frac{1}{\Gamma(2-\alpha)} \sum_{k=0}^{j-1} B_k \left[\frac{u_j^{k+1} - u_j^k}{(\Delta t)^{\alpha}}\right]; j = 1, ..., N. && (4.3)\\
B_k &= (j-k)^{1-\alpha} - (j-k-1)^{1-\alpha}. && (4.4)
\end{aligned}
$$

On the other hand, we have

$$u_{xx}(x_i, t_j) = \frac{1}{h^2} \left[u_{i+1}^j - 2u_i^j + u_{i-1}^j\right]; i = 1, ..., M-1. \tag{4.5}$$

Hence, the finite difference approximation for discretizing problem (3.1) is

$$
\begin{aligned}
\frac{1}{\Gamma(2-\alpha)} \sum_{k=0}^{j-1} B_k \frac{u_i^{k+1} - u_i^k}{(\Delta t)^{\alpha}} &= \frac{u_{i+1}^j - 2u_i^j + u_{i-1}^j}{h^2} - q_i u_i^j + c^j f_i, && (4.6)\\
u_i^0 &= \varphi_i, \quad i = 0, \ldots, M, && (4.7)\\
u_0^j &= u_M^j = 0, \quad j = 0, \ldots, N. && (4.8)
\end{aligned}
$$

Expanding the Caputo sum gives from the system (4.6) we get vector forms

$$
\begin{aligned}
\sum_{k=0}^{j-1} \left(u_i^{k+1} - u_i^k\right) B_k &= \left(u_i^1 - u_i^0\right) B_0 + (u_i^2 - u_i^1) B_1 + (u_i^3 - u_i^2) B_2 + ... + \left(u_i^j - u_i^{j-1}\right) B_{j-1} && (4.9)\\
&= -B_0 u_i^0 + (B_0 - B_1)\, u_i^1 + (B_1 - B_2)\, u_i^2 + ... + (B_{j-2} - B_{j-1})\, u_i^{j-1} + B_{j-1} u_i^j && (4.10)\\
&= -B_0 u_i^0 - \sum_{k=1}^{j-1} (B_k - B_{k-1})\, u_i^k + B_{j-1} u_i^j. && (4.11)
\end{aligned}
$$

Substituting in Eq.(4.6) and taking into consideration $B_{j-1} = 1$, let $r = (\Delta t)^{\alpha} \Gamma(2-\alpha)$, we get

$$-B_0 u_i^0 - \sum_{k=1}^{j-1} (B_k - B_{k-1})\, u_i^k + u_i^j = \frac{r}{h^2} \left[u_{i+1}^j - 2u_i^j + u_{i-1}^j\right] - r q_i u_i^j + r c^j f_i. \tag{4.12}$$

Introduce vectors

$$u^j = (u_1^j, \ldots, u_{M-1}^j)^T, \quad q = \mathrm{diag}(q_1, \ldots, q_{M-1}), \quad F = (f_1, \ldots, f_{M-1})^T,$$

and the tridiagonal matrix

$$A=\begin{pmatrix} -2 & 1 & 0 & \dots & 0 \\ 1 & -2 & 1 & \dots & 0 \\ 0 & 1 & -2 & \ddots & \vdots \\ \vdots & \ddots & \ddots & \ddots & 1 \\ 0 & \dots & 0 & 1 & -2 \end{pmatrix}_{(M-1)\times(M-1)},$$

a square matrix $(M-1)$, u^j is a vector solution of the order $(M-1)$, we get vector form

$$\frac{r}{h^2}Au^j-u^j-rEu^j=-\sum_{k=1}^{j-2}\left(B_k-B_{k-1}\right)u^k-B_0u^0-rc^jF; j=1,...,N. \tag{4.13}$$

Let $D=\frac{r}{h^2}A-I_{M-1}-rE$, where D is a matrix of the order $(M-1)$, and

$$E=\begin{pmatrix} q(x_1) & 0 & \cdots & 0 \\ 0 & q(x_2) & \cdots & 0 \\ \vdots & \ddots & \ddots & \vdots \\ 0 & \cdots & \cdots & q(x_{M-1}) \end{pmatrix}, \tag{4.14}$$

the diagonal matrix of the order $(M-1)$. Hence we get linear a system

$$Du^j=-\sum_{k=1}^{j-2}\left(B_k-B_{k-1}\right)u^k-B_0u^0-rc^j;\ j=1,...,N, \tag{4.15}$$

with $u^0=(u_1,u_2,...,u_{M-1})^T$. Let's create the method for predicting and fixing errors, first, using the output measurements $u(x_0,t)=E(t)$, we obtain

$$c(t)=\frac{D^\alpha E(t)-u_{xx}(x_0,t)+q(x_0)E(t)}{f(x_0)}. \tag{4.16}$$

The finite difference approximation of $c(t)$ is

$$c^j=\frac{E^j-\frac{1}{h^2}\left(u_{i+1}^j-2u_i^j+u_{i-1}^j\right)+q_iE^j}{f_i}, \tag{4.17}$$

where $E^j=D^\alpha u\left(\frac{1}{2},t\right)$.
The system of Equations (4.9) can be solved by the inversion matrix.

4.1. **Numerical examples.** To demonstrate the practical implementation of the method, we consider the following examples.

Example 4.1. Examine the following issue for $\alpha=0.25,\alpha=0.5,\alpha=0.75$

$${}^CD_t^\alpha u(x,t)-u_{xx}(x,t)+u(x,t)=c(t)\sin(\pi x); \qquad 0<x<1, 0<t<1. \tag{4.18}$$

$$u(x,0)=2\sin(\pi x); \qquad 0<x<1, \tag{4.19}$$

$$u(0,t)=u(1,t)=0; \qquad 0<t<1. \tag{4.20}$$

The exact solutions of this problem for $\alpha=0.25,\alpha=0.5$ and $\alpha=0.75$ are respectively

$$\{c(t),u(x,t)\}=\left\{1.223t^{2.25}+1.089t^{0.75}+\left(\pi^2+1\right)\left(t^{\frac{9}{4}}+t+2\right),\left(t^{\frac{9}{4}}+t+2\right)\sin(\pi x)\right\}. \tag{4.21}$$

TABLE 1. Numerical results for $\alpha = 0.25$.

t	Numerical solution	Exact solution	Error
0	2.0000	2.0000	00000
0.0250	2.0252	2.0258	0.0006
0.0500	2.0512	2.0516	0.0004
0.0750	2.0779	2.0781	0.0003
0.1000	2.1056	2.1055	0.0001
0.1250	2.1343	2.1338	0.0006
0.1500	2.1640	2.1632	0.0008
0.1750	2.1833	2.1850	0.0017

TABLE 2. Numerical results for $\alpha = 0.5$.

t	Numerical solution	Exact solution	Error
0	2.0000	2.0000	00000
0.0250	2.0257	2.0251	0.0006
0.0500	2.0513	2.0506	0.0007
0.0750	2.0771	2.0765	0.0006
0.1000	2.1040	2.1032	0.0008
0, 1250	2.1314	2.1305	0.0009
0.1500	2.1597	2.1587	0.0008
0.1750	2.1888	2.1887	0.0001

TABLE 3. Numerical results for $\alpha = 0.75$.

t	Numerical solution	Exact solution	Error
0	2.0000	2.0000	00000
0.0250	2.0250	2.0251	0.0001
0.0500	2.0503	2.0505	0.0002
0.0750	2.0758	2.0762	0.0004
0.1000	2.1018	2.1025	0.0007
0.1250	2.1283	2.1393	0.0010
0.1500	2.1554	2.1568	0.0013
0.1750	2.1833	2.1850	0.0017

$$\{c(t), u(x,t)\} = \left\{ \frac{1}{16\sqrt{\pi}}(15t^2\pi + 32\sqrt{t}) + (\pi^2+1)(t^{\frac{5}{2}} + t + 2), (t^{\frac{5}{2}} + t + 2)\sin(\pi x) \right\}. \tag{4.22}$$

$$\{c(t), u(x,t)\} = \left\{ \frac{\Gamma(3.5)}{\Gamma(2.75)} t^{1.75} + \frac{\Gamma(2)}{\Gamma(1.25)} t^{0.25} + \left(\pi^2+1\right)\left(t^{\frac{11}{4}} + t + 2\right), (t^{\frac{11}{4}} + t + 2)\sin(\pi x) \right\}. \tag{4.23}$$

The following tables illustrates the differences between the numerical and exact solutions, demonstrating the accuracy of the $L1$ method, for the step sizes $h = 0.025, \Delta t = 0.025, x = 0.5$. Additionally, the L_∞ and L_2 norms of the error are given in the following table These figures clearly demonstrate excellent agreement between the numerical and exact solutions for $c(t)$ and $u(x,T)$. To further demonstrate the effectiveness of the proposed method, we present the following example.

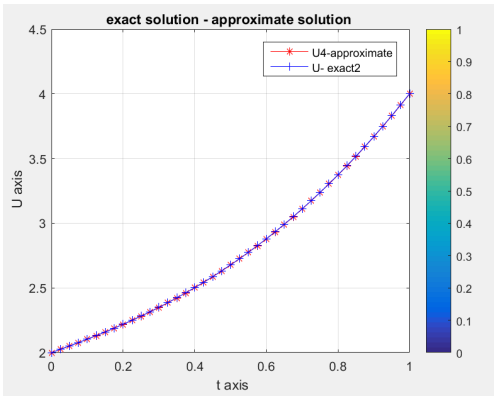

(A) The exact and numerical solution of $u = (0.5, t)$.

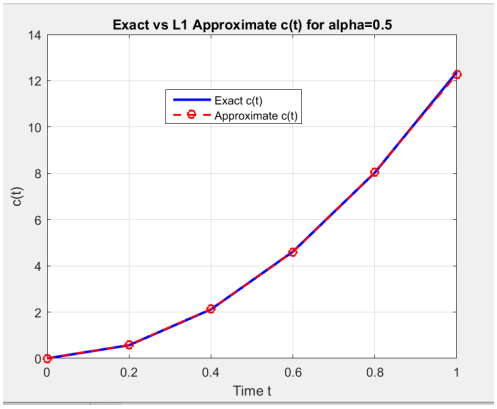

(B) The exact and numerical solution of $c(t)$.

FIGURE 1. The exact and numerical solution of $u = (0.5, t)$ and $c(t)$.

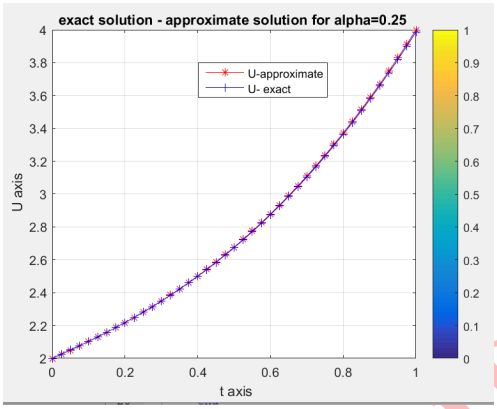

(A) The exact and numerical solution of $u = (0.25, t)$.

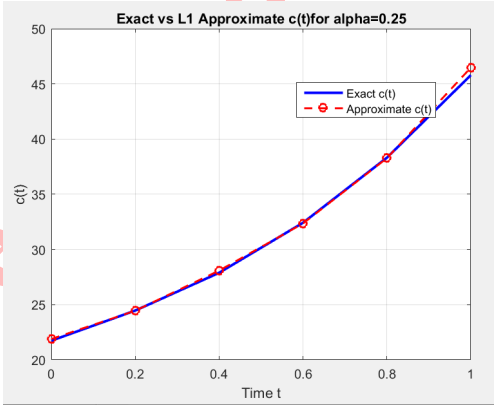

(B) The exact and numerical solution of $c(t)$.

FIGURE 2. The exact and numerical solution of $u = (0.25, t)$ and $c(t)$.

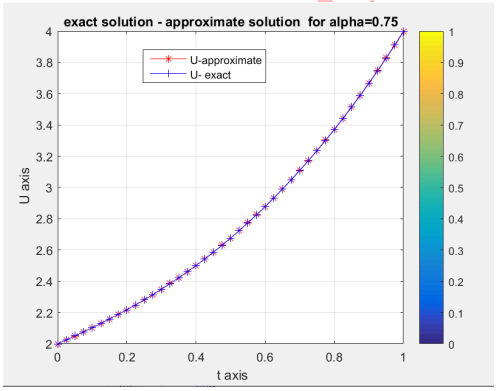

(A) The exact and numerical solution of $u = (0.75, t)$.

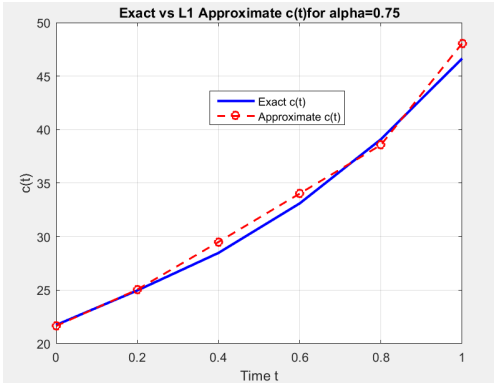

(B) The exact and numerical solution of $c(t)$.

FIGURE 3. The exact and numerical solution of $u = (0.75, t)$ and $c(t)$.

TABLE 4. L_∞ and L_2 norms of error for Example 4.1.

α	L_∞ error	L_2 error
0.25	0.0103	0.0452
0.5	0.0020	0.0088
0.75	0.0123	0.0279

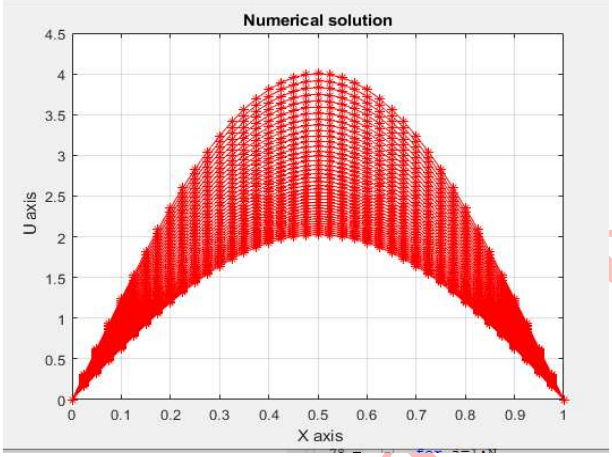

FIGURE 4. The numerical solution $U^j, j = 1, ..., 40$.

Example 4.2. Examine the following issue for $\alpha = 0.25, \alpha = 0.5$, and $\alpha = 0.75$

$$ {}^{C}D_t^{\alpha} u(x,t) - u_{xx}(x,t) + u(x,t) = c(t)\sin(\pi x), \qquad 0 < x < 1, < t < 1. \tag{4.24} $$

$$ u(x,0) = 0; \qquad 0 < x < 1, \tag{4.25} $$

$$ u(0,t) = u(1,t) = 0; \qquad 0 < t < 1. \tag{4.26} $$

The exact solutions of this problem for $\alpha = 0.25, \alpha = 0.5$ and $\alpha = 0.75$ are respectively

$$ \{c(t), u(x,t)\} = \left\{ \frac{2}{\Gamma(2.75)} t^{1.75} + (\pi^2+1)t^2, t^2 \sin(\pi x) \right\}. \tag{4.27} $$

$$ \{c(t), u(x,t)\} = \left\{ \frac{8}{3\sqrt{\pi}} t^{1.5} + (\pi^2+1)t^2, t^2 \sin(\pi x) \right\}. \tag{4.28} $$

$$ \{c(t), u(x,t)\} = \left\{ \frac{2}{\Gamma(2.25)} t^{1.25} + (\pi^2+1)t^2, t^2 \sin(\pi x) \right\}. \tag{4.29} $$

The following tables illustrates the differences between the numerical and exact solutions, demonstrating the accuracy of the $L1$ method, for the step sizes $h = 0.02, \Delta t = 0.01, x = 0.5$.

TABLE 6. Numerical results for $\alpha = 0.5$.

t	Numerical solution	Exact solution	Error
0	2.0000	2.0000	00000
0.0100	0.0001	0.0001	00000
0.0200	0.0004	0.0004	00000
0.0300	0.0009	0.0009	00000
0.0400	0.0016	0.0016	00000
0.0500	0.0025	0.0025	00000
0.0600	0.0036	0.0036	00000
0.0700	0.0049	0.0049	00000

TABLE 7. Numerical results for $\alpha = 0.75$.

t	Numerical solution	Exact solution	Error
0	2.0000	2.0000	00000
0.0100	0.0001	0.0001	00000
0.0200	0.0004	0.0005	0.0001
0.0300	0.0009	0.0010	0.0001
0.0400	0.0016	0.0017	0.0001
0.0500	0.0025	0.0026	0.0001
0.0600	0.0036	0.0037	0.0001
0.0700	0.0049	0.0050	0.0001

TABLE 8. L_∞ and L_2 norms of error for Example 4.2.

α	L_∞ error	L_2 error
0.25	0.0035	0.0168
0.5	$3.0207e^{-4}$	0.0015
0.75	0.0028	0.0146

TABLE 5. Numerical results for $\alpha = 0.25$.

t	Numerical solution	Exact solution	Error
0	2.0000	2.0000	00000
0.0100	0.0001	0.0001	00000
0.0200	0.0004	0.0004	00000
0.0300	0.0009	0.0009	00000
0.0400	0.0016	0.0016	00000
0.0500	0.0025	0.0025	00000
0.0600	0.0036	0.0036	00000
0.0700	0.0049	0.0049	00000

Additionally, the L_∞ and L_2 norms of the error are given in the following table The excellent match observed in these figures between the numerical and exact solutions for $c(t)$ and $u(x, T)$ validates the effectiveness of the proposed approach.

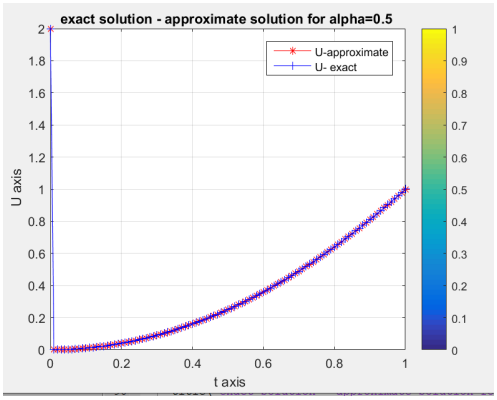

(A) The exact and numerical solution of $u = (0.5, t)$.

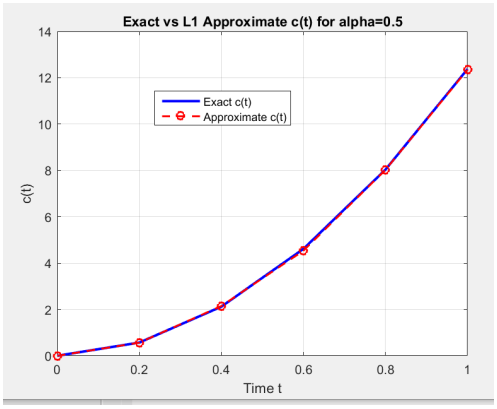

(B) The exact and numerical solution of $c(t)$.

FIGURE 5. The exact and numerical solution of $u = (0.5, t)$ and $c(t)$.

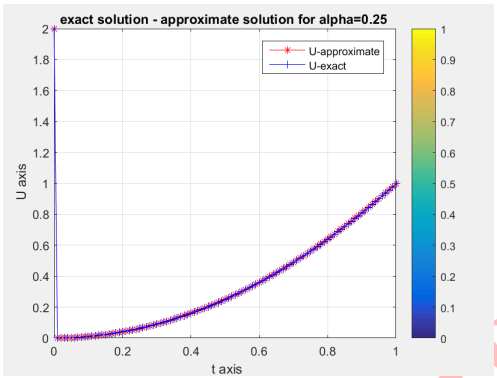

(A) The exact and numerical solution of $u = (0.25, t)$.

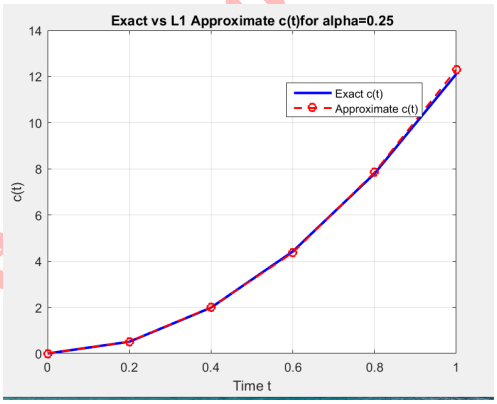

(B) The exact and numerical solution of $c(t)$.

FIGURE 6. The exact and numerical solution of $u = (0.25, t)$ and $c(t)$.

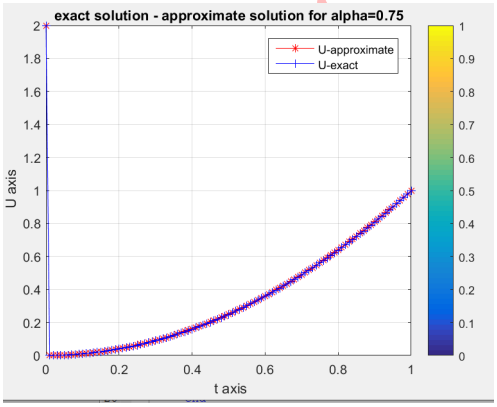

(A) The exact and numerical solution of $u = (0.75, t)$.

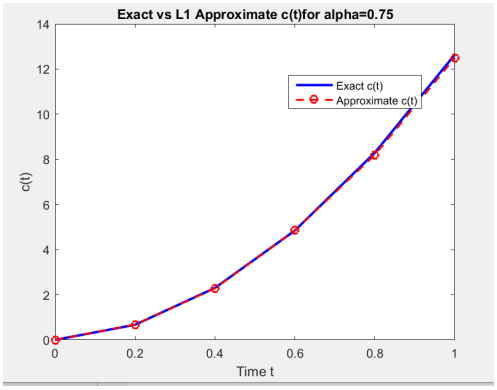

(B) The exact and numerical solution of $c(t)$.

FIGURE 7. The exact and numerical solution of $u = (0.75, t)$ and $c(t)$.

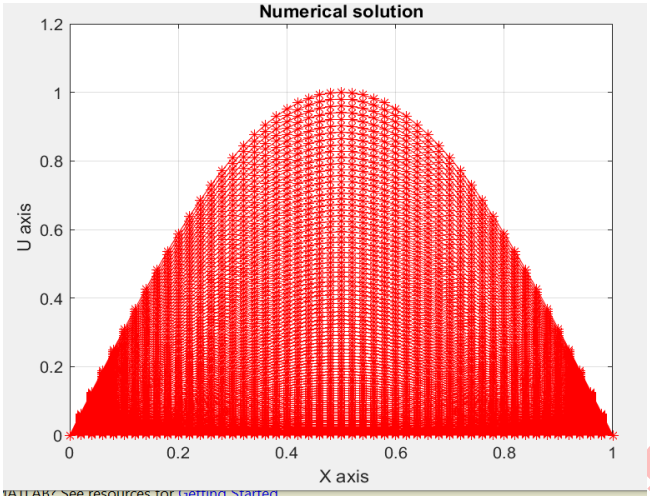

FIGURE 8. The numerical solution $U^j, j = 1, ..., 100$.

5. Conclusion

The numerical scheme for solving the temporal fractional diffusion problem by the explicit finite difference approach is presented in this study. Through the use of variable separation and input-output mapping in the analysis of fractional parametric equation inversion problems, this work expands our understanding of Fourier methods. The examples we provided are intended to illustrate the performance and accuracy of this approach. Building more efficient algorithms is also a goal of our future work. We utilized the algebraic system Maple 15 for the numerical algorithm, and Matlab 2018 was employed to create the solution's graphic.

Acknowledgements

We would like to express gratitude to the reviewers and the editor for their valuable feedback and contributions to the improvement of this work.

References

[1] M. Abbaszadeh and M. Dehghan, *Meshless upwind local radial basis function-finite difference technique to simulate the time-fractional distributed-order advection–diffusion equation*, Eng. Comput., *37*(2) (2021), 873–889.
[2] M. Abbaszadeh and M. Dehghan, *Error estimate of virtual element approximation for loaded time-fractional Hallaire's equation*, J. Appl. Math. Comput., *71*(3) (2025), 4475–4502.
[3] R. Atmania and L. Settara, *An inverse source time-fractional diffusion problem via an input-output mapping*, Proyecciones (Antofagasta), *42*(5) (2023), 1105–1127.
[4] R. Atmania and L. Settara, *An inverse source Cauchy-weighted time-fractional diffusion problem*, Hacet. J. Math. Stat., *53*(5) (2023), 1354–1367.
[5] D. Altan Koç and G. Mustafa, *Numerical approach for solving time fractional diffusion equation*, Int. J. Optim. Control: Theor. Appl., *7*(3) (2017), 2146–0957.
[6] M. Dehghan and M. Abbaszadeh, *An efficient technique based on finite difference/finite element method for solution of two-dimensional space/multi-time fractional Bloch–Torrey equations*, Appl. Numer. Math., *131* (2018), 190–206.
[7] H. W. Engl, M. Hanke, and A. Neubauer, *Regularization of Inverse Problems*, Kluwer Acad. Publ., Dordrecht, Boston, London, 1996.
[8] R. Faizi and R. Atmania, *An inverse source problem of a semilinear time-fractional reaction–diffusion equation*, Appl. Anal., *102*(11) (2023), 2939–2959.

[9] R. Faizi and R. Atmania, *An inverse source problem for a generalized time fractional diffusion equation*, Eurasian J. Math. Comput. Appl., *10*(1) (2022), 26–39.
[10] G. H. Gao, Z. Z. Sun, and H. W. Zhang, *A new fractional numerical differentiation formula to approximate the Caputo fractional derivative and its applications*, J. Comput. Phys., *259* (2014), 33–50.
[11] A. Ghoreyshi, M. Abbaszadeh, M. A. Zaky, and M. Dehghan, *Two high-order numerical schemes based on the Lagrange polynomials for solving a distributed-order time-fractional partial integro-differential equation on non-rectangular domains*, J. Appl. Math. Comput., *71*(5) (2025), 7271–7311.
[12] A. Ghoreyshi, M. Abbaszadeh, M. A. Zaky, and M. Dehghan, *Finite block method for nonlinear time-fractional partial integro-differential equations: Stability, convergence, and numerical analysis*, Appl. Numer. Math., *214* (2025), 82–103.
[13] J. H. He, *Approximate analytical solution for seepage flow with fractional derivatives in porous media*, Comput. Methods Appl. Mech. Eng., *167*(1–2) (1998), 57–68.
[14] V. Isakov, *Inverse Problems for Partial Differential Equations*, Springer, New York, 2006.
[15] S. I. Kabanikhin, *Definitions and examples of inverse and ill-posed problems*, Inverse Probl. Sci. Eng., *16*(4) (2008), 317–357.
[16] M. I. Ismailov, F. Kanca, and D. Lesnic, *Determination of a time dependent heat source under nonlocal boundary and integral overdetermination conditions*, Appl. Math. Comput., *218*(8) (2011), 4138–4146.
[17] A. A. Kilbas, H. M. Srivastava, and J. J. Trujillo, *Theory and Applications of Fractional Differential Equations*, Elsevier, 2006.
[18] M. Kurulay and M. Bayram, *Approximate analytical solution for the fractional modified KdV by differential transform method*, Commun. Nonlinear Sci. Numer. Simul., *15*(7) (2010), 1777–1782.
[19] Z. Li and M. Yamamoto, *Uniqueness for inverse problems of determining orders of multi-term time-fractional derivatives of diffusion equation*, Appl. Anal., *94*(3) (2015), 570–579.
[20] Y. Lin and C. Xu, *Finite difference/spectral approximations for the time-fractional diffusion equation*, J. Comput. Phys., *225*(2) (2007), 1533–1552.
[21] Y.-H. Lin and H. Liu, *Inverse problems for fractional equations with a minimal number of measurements*, arXiv:2203.03010 (2022).
[22] A. Oulmelk, L. Afraites, A. Hadri, M. A. Zaky, and A. S. Hendy, *Alternating direction multiplier method to estimate an unknown source term in the time-fractional diffusion equation*, Comput. Math. Appl., *156*(1) (2024), 195–206.
[23] E. Ozbilge, A. Demir, F. Kanca, and E. Özbilge, *Determination of the unknown source function in time fractional parabolic equation with Dirichlet boundary conditions*, Appl. Math. Inf. Sci., *10*(1) (2016), 283–289.
[24] I. Podlubny, *Fractional Differential Equations*, Elsevier, 1998.
[25] B. Jin and W. Rundell, *An inverse problem for a one-dimensional time-fractional diffusion problem*, Inverse Probl., *28*(7) (2012), 075010.
[26] A. N. Tikhonov and V. A. Arsenin, *Solutions of Ill-Posed Problems*, Winston and Sons, Washington, DC, 1977.
[27] C. A. Xinlin and H. Y. Liu, *Determining a fractional Helmholtz equation with unknown source and scattering potential*, Commun. Math. Sci., *17*(7) (2019), 1861–1876.
[28] Z. Zhang, *An undetermined coefficient problem for a fractional diffusion equation*, Inverse Probl., *32*(1) (2015), 015011.